Protein Corona-Mediated Mitigation of Cytotoxicity of Graphene Oxide

Wenbing Hu, Cheng Peng, Min Lv, Xiaoming Li, Yujie Zhang, Nan Chen, Chunhai Fan,* and Qing Huang*

Laboratory of Physical Biology, Shanghai Institute of Applied Physics, Chinese Academy of Sciences, Shanghai 201800, People's Republic of China

ABSTRACT Graphene is a single layer of sp^2-bonded carbons that has unique and highly attractive electronic, mechanical, and thermal properties. Consequently, the potential impact of graphene and its derivatives (e.g., graphene oxide, GO) on human and environmental health has raised considerable concerns. In this study, we have carried out a systematic investigation on cellular effects of GO nanosheets and identified the effect of fetal bovine serum (FBS), an often-employed component in cell culture medium, on the cytotoxicity of GO. At low concentrations of FBS (1%), human cells were sensitive to the presence of GO and showed concentration-dependent cytotoxicity. Interestingly, the cytotoxicity of GO was greatly mitigated at 10% FBS, the concentration usually employed in cell medium. Our studies have demonstrated that the cytotoxicity of GO nanosheets arises from direct interactions between the cell membrane and GO nanosheets that result in physical damage to the cell membrane. This effect is largely attenuated when GO is incubated with FBS due to the extremely high protein adsorption ability of GO. The observation of this FBS-mitigated GO cytotoxicity effect may provide an alternative and convenient route to engineer nanomaterials for safe biomedical and environmental applications.

KEYWORDS: graphene oxide · cytotoxicity · protein adsorbability · cell membrane damage

Carbon nanomaterials are a family of important nanomaterials[1] with many unique properties that represent diverse application potential,[2−9] including in the biomedical field.[10−13] In particular, fullerene, nanodiamond, and carbon nanotubes (CNTs) have been extensively employed as intracellular agents for drug delivery,[14] gene regulation,[15] and imaging.[16−18] Graphene is a newly discovered two-dimensional carbon nanomaterial with a single layer of sp^2-bonded carbon that has attracted intense interest,[19−21] due to its fascinating electronic, mechanical, and thermal properties.[22−24] While many breakthroughs have been made toward the nanoelectronic applications for graphene (*e.g.*, ultrafast transistors[25] and ambipolar memory device[26]), biological studies on graphene and its derivatives (*e.g.*, graphene oxide (GO), reduced graphene oxide) have only recently become the subject of active investigation.[27,28] Several groups have reported that functionalized GO undergoes high *in vivo* uptake in healthy cells and tumors and then could serve as nanocargos to effectively deliver insoluble drugs,[29−31] nucleic acids,[32,33] and other molecules[34] into cells for bioimaging and therapeutic purposes.

Given the exceptional promise of biomedical applications for graphene and GO, it is critically important that a systematic evaluation of their potential risk to human health be carried out.[35] Generally speaking, carbon-based nanomaterials are regarded as "safe" since the carbon element is inherently compatible with living systems. Indeed, a range of carbon nanomaterials,[36,37] including functionalized graphene,[29,30,38−40] have exhibited little cytotoxicity in studies involving living cell lines. Recent studies showed that the dose-dependent cytotoxicity of GO during the 24 h incubation time was attributed to the generation of reactive oxygen species (ROS),[41,42] while nonfunctionalized GO was capable of killing bacteria *via* cell membrane damage.[43,44] Our previous studies revealed that nonfunctionalized GO was capability of killing bacteria, while minimally perturbing mammalian cells.[44] Other studies also suggested that graphene nanomaterials functionalized by macromolecules (chitosan,[45] tween,[39] artificial peroxidase,[46] PEI,[47] components of cell medium[38,48,49]) or PEG[29,30] demonstrated excellent biocompatibility. These studies clearly suggested complex interactions between graphene nanomaterials and cells. Consequently, we herein carried out systematic investigations on the interactions between GO nanosheets and mammalian cells and reported our finding of the serum-mitigated cytotoxicity of GO.

RESULTS AND DISCUSSION

GO nanosheets prepared *via* the modified Hummers method[50] exhibited a thickness of ~1.0 nm under atomic force microscopy (AFM) (Figure 1b), characteristic of a single layer of 2-D nanosheets.[51] Interestingly, when GO was incubated in the commonly used cell culture RPMI 1640 medium that is supplemented with fetal

* Address correspondence to fchh@sinap.ac.cn; huangqing@sinap.ac.cn.

Received for review January 3, 2011 and accepted April 18, 2011.

Published online April 18, 2011
10.1021/nn200021j

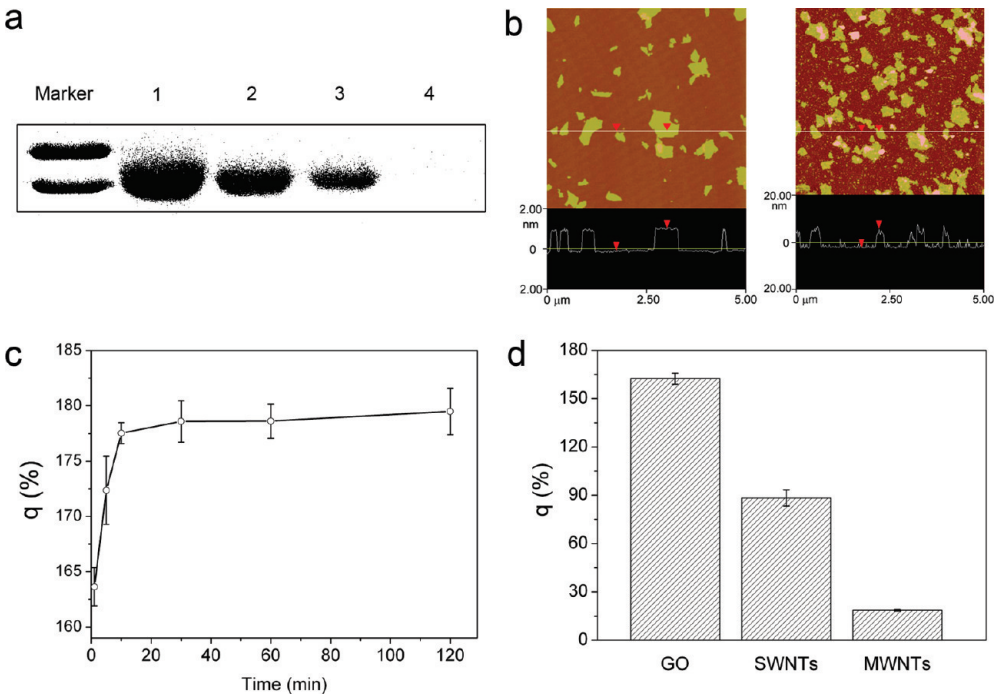

Figure 1. Characterization of interaction of GO with FBS proteins. (a) SDS-PAGE of FBS proteins in the supernatant after centrifugation. 50 μL of 10% (v/v) FBS solution was incubated with different amounts of GO (the amount of GO from lane 1 to land 4 was 0, 40, 80, and 100 μg, respectively) for 2 h at 37 °C. The molecular weight of Marker was 72 kD (top) and 55 kD (bottom), respectively. (b) AFM images of GO (left) and FBS-coated GO nanosheets (right). 100 μL of GO (1 mg/mL) was incubated with 200 μL of RPMI 1640 medium (10% v/v FBS) for 2 h at 37 °C, and then FBS-caoted GO was resuspended in Milli-Q water after centrifugation. (c) FBS protein loading ratio on the surfaces of GO at different incubation times. The GO was incubated with FBS proteins at 37 °C for 1, 5, 10, 30, 60, and 120 min. Then the amount of FBS proteins in the supernatant was determined *via* the Bradford method after centrifugation. (d) BSA loading capability of GO, SWNTs, and MWNTs. After incubation with BSA solution at 37 °C for 2 h, the mixture was centrifugated. Then the amount of BSA in the supernatant was determined. The capability of BSA loading was evaluated by the following: $q = (W_{Total} - W_{Sup})/(W_{GO}) \times 100\%$ (W_{Total}, W_{Sup}, W_{GO} represent the total amount of protein, the amount of protein in the suspension, and the quantity of GO, respectively).

bovine serum (FBS) for 2 h, the amount of FBS proteins in the supernatant decreased along with the increase of GO concentration (Figure 1a), suggesting the existence of strong interactions between GO and FBS proteins. The thickness of GO in RPMI 1640 medium substantially increased to the range 4.0−18.0 nm (Figure 1b). This observations revealed that a large amount of proteins had coated the surfaces of the GO nanosheets (designated as FBS-coated GO). Additionally, GO−FBS protein binding reached equilibrium within 30 min (Figure 1c). In order to further study the interactions, we explored the adsorption ability of GO nanosheets by measuring the amount of a model protein, bovine serum albumin (BSA), adsorbed to GO. As shown in Figure 1d, 1 mg of GO nanosheets was able to adsorb ∼1.6 mg of BSA. This loading capacity was respectively ∼9-fold and ∼1.8-fold higher than that of BSA to two well-known nanomaterials with high protein adsorption ability, namely, multiwalled carbon nanotubes (MWNTs) and single-walled carbon nanotubes (SWNTs). These data suggested that GO nanosheets possessed exceptionally high adsorption capability for abundant proteins in the FBS medium, which arose form the special 2-D nanostructure that provides ultrahigh surface-to-volume ratios. Proteins might be adsorbed to the surfaces of GO *via* both electrostatic and hydrophobic interactions. In addition, GO possessed many surface defects that could serve as binding sites for proteins, while defects of CNTs usually existed at both ends rather than the walls. This difference could contribute to the observed different protein adsorption ability of GO and CNTs.

We employed the classic MTT viability assays to evaluate and compare the cytotoxicity of GO nanosheets and two types of carbon nanotubes (SWNTs and MWNTs). A549 (adenocarcinomic human alveolar basal epithelial) cells were incubated in the presence of either GO or MWNTs for 24 h, and the dose-dependent cytotoxicity of both was observed (Figure 2a). As a general trend, the cytotoxicity of both nanomaterials was mild with a ∼50% decrease in the metabolic activity for GO and ∼30% for MWNTs, even at the high concentration of 100 μg/mL. Of note, the cytotoxicity of GO was slightly higher (∼10−20%) than that of MWNTs.

Interestingly, the cytotoxicity of GO was not found to be strongly dependent on the duration of incubation time. As shown in Figure 2b, while there was a small difference (5−10%) in the dose-dependent metabolic

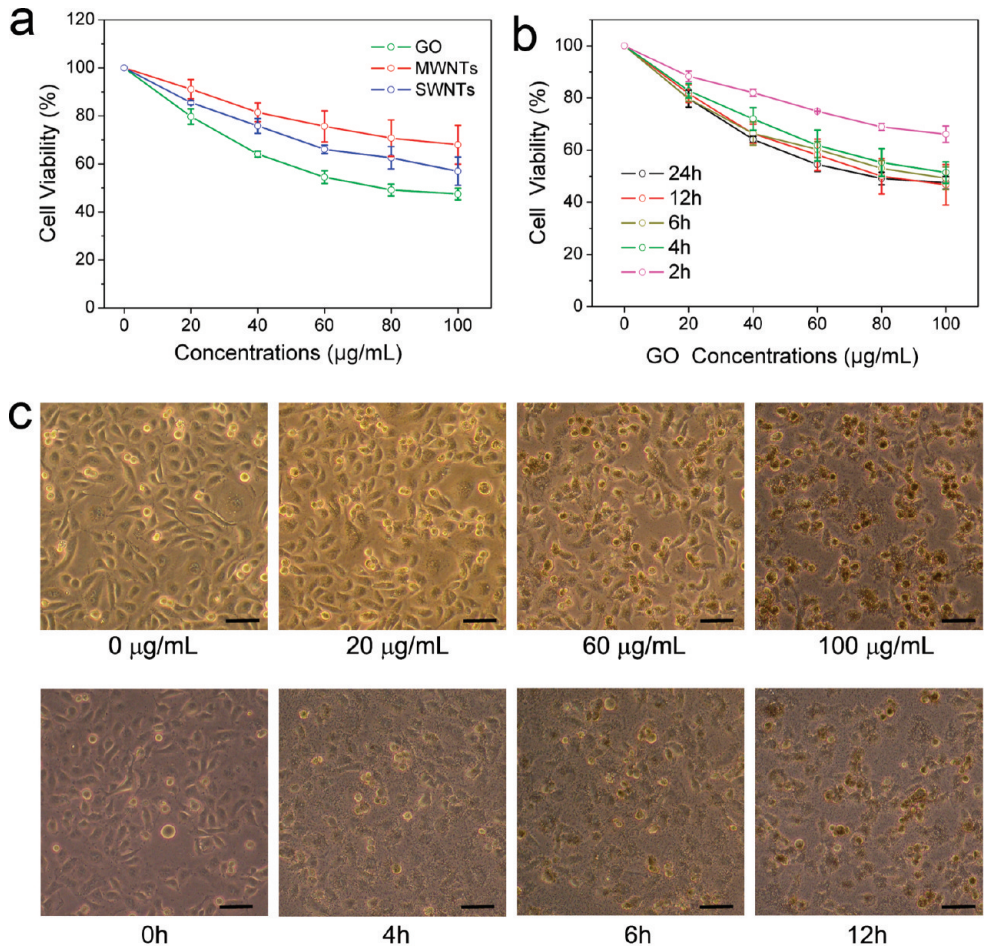

Figure 2. Cytotoxicity of GO nanosheets against A549 cells in complete RPIM 1640 medium (10% v/v FBS). (a) Comparison of the cytotoxic effects of 100 μg/mL carbon nanotubes (MWNTs and SWNTs) with GO nanosheets on A549 cells for 24 h, based on MTT assays. (b) Cell viability of A549 cells treated with GO nanosheets at different concentrations and incubation times. (c) Morphology of A549 cells treated with different concentrations of GO nanosheets for 24 h (top) and 100 μg/mL GO nanosheets for a series of incubation times (bottom). The scale bar is 20 μm.

activity curves of the 2 and 4 h incubation times, the metabolic activity of cells was almost identical, and this characteristic remained when the incubation time was prolonged to 24 h. The number of live cells and their morphological change further confirmed the absence of a time-dependent mechanism for GO-induced cytotoxicity (Figure 2c), implying that GO killed cells only upon initial interaction. It was presumable that subsequent incubation in the cell medium passivated GO and mitigated its cytotoxicity. By contrast, previous studies revealed that MWNTs exhibited time-dependent cytotoxicity,[52] possibly resulting from poorer protein adsorption ability of MWNTs as compared to GO.

We reasoned that this mitigation behavior arose from the high protein adsorption ability of GO[53−55] and the presence of abundant proteins in FBS of the RPMI 1640 medium used in our study. We then measured the viability of GO-treated A549 cells for 2 h in RPMI 1640 medium supplemented with conventional (10%) and low (1%) concentrations of FBS. The medium with 10% FBS was associated with a slight increase (5−10%) in cell viability (Figure 3a). Of note, GO substantially coagulated in the presence of FBS-free medium;[47] thus it was not employed for the cytotoxicity studies. However, the relatively small mitigation effect that accompanied the 10-fold decrease in the FBS concentration suggested that uncoated GO could instantly kill a significant amount of cells upon interaction with the cells. Significantly, when GO was precoated with FBS and then incubated with cells in the medium with 10% FBS, the cytotoxic effect was largely reduced; nearly 100% survival was achieved with 20 μg/mL FBS-coated GO and ~90% with 100 μg/mL FBS-coated GO. Similar trends were observed with longer incubation times (4 and 6 h; Figure 3b) and GO covered by BSA (Figure S2). These data further suggested that the cytotoxicity of GO was a result of the initial direct interactions of GO with cells. Previous studies have revealed that BSA might not be the primary component for the formation of a protein corona on the surface of nanomaterials.[56,57] However, the similarity in the observed cytotoxicity of FBS- and BSA-coated GO suggested that the main function of protein

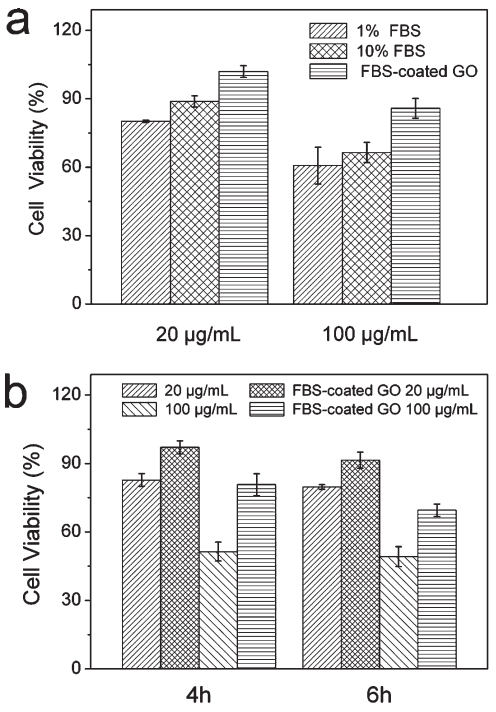

Figure 3. Cytotoxic effect of FBS on cytotoxicity of GO nanosheets. (a) Cell viability of A549 cells treated with GO nanosheets (20 μg/mL, 100 μg/mL) dispersed in RPMI medium 1640 containing various concentrations of FBS for 2 h. (b) Cell viability of A549 cells treated with GO (10% FBS) and FBS-coated GO nanosheets for 4 and 6 h.

adsorption might come from the impedance of the GO surfaces from their direct interactions with cells; thus the component of the protein corona did not contribute significantly to the cytotoxicity.

We further studied the temperature effect on the cytotoxicity of GO. At both 4 and 37 °C, viability of cells exposed to GO nanosheets was much lower than that of cells treated with FBS-coated GO nanosheets. This finding complemented the hypothesis that FBS was able to reduce the cytotoxicity of GO nanosheets *via* weakening of the interactions between GO and cells. A549 cells treated with FBS-coated GO nanosheets did not exhibit any cytotoxic effects at either 4 or 37 °C (Figure 4); however, in the FBS-free RPMI 1640 medium the viability of 20 μg/mL GO-treated A549 cells at 4 °C was ~30% higher than that at 37 °C (Figure 4), suggesting that incubation temperature could play an important role in mitigating the interactions between A549 cells and GO nanosheets. Since cell membranes tend to be less fluidic and have lower permeability at lower temperatures, our results suggested that relationships may exist between the cytotoxic mechanisms of GO and the integrity of cell membranes.

Transmission electron microscopic (TEM) imaging was employed to obtain direct evidence for the distinct morphological changes elicited upon A549 cells being exposed to GO (Figure 5). After A549 cells

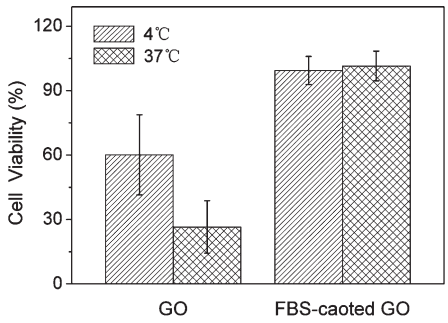

Figure 4. Viability of A549 cells treated with GO nanosheets and FBS-coated GO nanosheets at 4 and 37 °C. The A549 cells were incubated with 20 μg/mL GO or FBS-coated GO at 4 and 37 °C for 2 h; then the viability was determined *via* MTT assay.

were incubated with 100 μg/mL GO in 1% FBS medium at 37 °C for 2 h, the membrane of treated A549 cells had become obviously severed, with the outflow of cytoplasm indicating irreversible cell damage. GO nanosheets were also observed in the cytoplasm (Figure 5a–d). In contrast, A549 cells that had been treated with FBS-coated GO remained viable with their membrane integrity intact (Figure 5e,f). Thus, TEM imaging demonstrated that uncoated GO destroys cell membranes and directly induces cell death, an effect that is eliminated by precoating of GO with FBS.

We proposed that the cytotoxicity of GO nanosheets occurred as a result of physical damage to the cell membrane, which was induced by direct interactions between the cell membrane and GO nanosheets. Previous studies on the cytotoxicity of MWNTs/SWNTs have suggested three mechanisms underlying this event: oxidative stress,[58,59] metal toxicity,[60,61] and physical piercing causing rupture.[62] Interestingly, we discovered that the cytotoxicity of GO nanosheets occurred mostly during the initial contact stage of GO and cells and was independent of exposure duration. This observation largely excluded the contribution of an oxidative stress mechanism since that is a time-dependent process. In addition, there were essentially no metal catalysts involved in the synthesis of GO (see Experimental Section, Preparation of GO Nanosheets). These two mechanisms, thus, could not account for the cytotoxic effects of GO on human cells. On the other hand, previous molecular dynamics[63] and TEM[64] studies have revealed that highly dispersed single SWNTs were able to cross cell membranes and enter the intracellular space. Recent studies have also suggested that GO and SWNTs can cause physical damage to the outer membrane of *E. coli* bacteria, resulting in the release of intracellular components.[43,44,65,66] Our temperature studies provided additional evidence of physical damage of the cell membrane. Despite the presence of the evidence, we emphasize that the principal mechanism

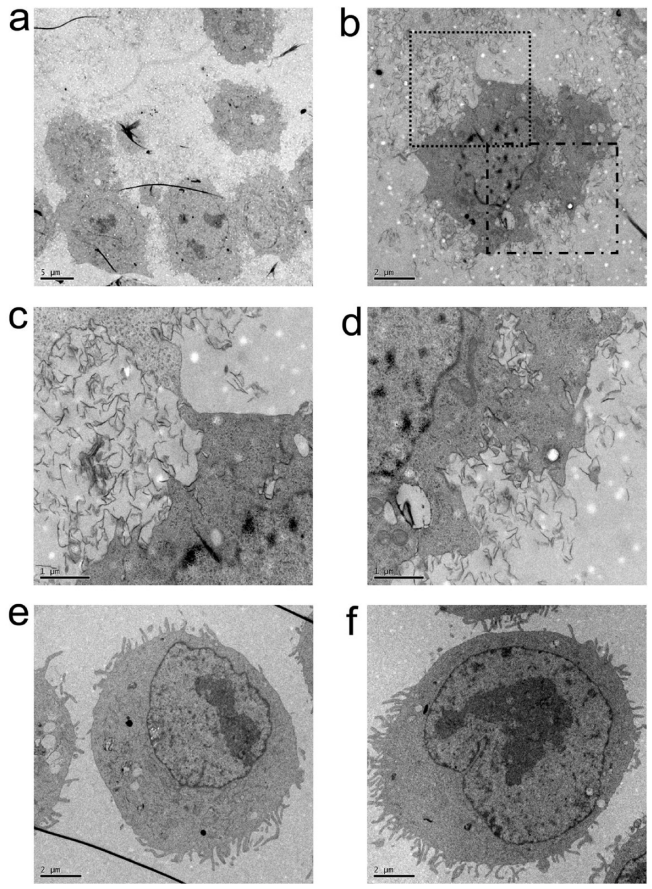

Figure 5. TEM images of A549 cells treated with 100 μg/mL GO nanosheets (a, b) and FBS-coated GO nanosheets (e, f) at 37 °C for 2 h. (c, d) Magnified regions of (b) showing interactions between GO nanosheets and A549 cells.

responsible for the observed cytotoxicity of GO has to be the subject of thorough investigations.

It is worthwhile to note that the observed FBS-mitigated cytotoxicity has important implications for the developed and future applications. First, nanomaterials can easily form "coronas" with proteins in biological systems;[56,57,67,68] thus it is important to consider contextual effects when evaluating the safety of nanomaterials.[69,70] Second, since FBS is usually present in cell culture medium, GO is fairly safe for use in most medium-based cellular studies, as has been previously reported (despite the undefined nature of the FBS role).[29−31,47] Third, mitigation of nanomaterial-induced toxicity is a major concern in the field of nanotechnology.[71] Our observations of FBS-mitigated GO cytotoxicity may provide an alternative and convenient method by which to engineer nanomaterials for safe biomedical and environmental applications.

EXPERIMENTAL SECTION

Preparation of GO Nanosheets. GO nanosheets were prepared from purified natural graphite by using the modified Hummers method,[50] resulting in a colloidal suspension of GO sheets. In a typical experiment, graphite powder (4 g) was added to a mixture of 24 mL of concentrated H_2SO_4, 8 g of $K_2S_2O_8$, and 8 g of P_2O_5. The mixture was heated to 80 °C and maintained with stirring for 5 h. The resultant dark blue mixture was thermally isolated and allowed to slowly cool to room temperature, over a period of 6 h. The cooled mixture was then diluted to 300 mL and filtered through a 0.22 μm membrane (Generay Biotech Co., Ltd., Shanghai, China). The filtrate was dried overnight at 60 °C. The preoxidized graphite powder (2 g) was added to 92 mL of cold H_2SO_4 (0 °C), followed by 12 g of $KMnO_4$ being added gradually with stirring in an ice bath. After stirring for 15 min, 2 g of $NaNO_3$ was added to the mixture, and stirring was continued for an additional 2 h at 35 °C, after which distilled water (200 mL) was added. The reaction was terminated by addition of 10 mL of 30% H_2O_2 and 570 mL of distilled water. For purification, the mixture was first washed with 1:10 HCl and then with Milli-Q water. The graphite oxide product was resuspended in water to form a brown dispersion, which was subjected to dialysis in order to remove residual metal ions and acids. The purified graphite oxide dispersion was sonicated for 1.5 h at 300 W to exfoliate the graphene oxide; unexfoliated graphene oxide was removed by centrifugation (3000 rpm, 5 min). The final graphene oxide products were then characterized with atomic force microscopy.

Characterization of Interaction of GO with FBS Proteins. A 50 μL amount of 10% (v/v) FBS solution was mixed with different amounts of GO (0, 40, 80, 100 μg), and then the mixture was kept for 2 h at 37 °C. After centrifugation at ~19000*g* for 10 min, 10 μL of the supernatant was applied to sodium dodecyl sulfate polyacrylamide gel electrophoresis (SDS-PAGE).

A 100 μL portion of GO suspension at 1 mg/mL concentration was mixed with 200 μL of RPMI 1640 medium supplemented with 10% (v/v) FBS at 37 °C for 2 h. After centrifugation at ~19000*g* for 10 min, the conjugates were resuspended in Milli-Q water and imaged *via* AFM.

The GO was incubated with FBS proteins at 37 °C for 1, 5, 10, 30, 60, and 120 min. After centrifugation, the amount of FBS proteins in the supernatant was determined *via* Bradford Protein Assay Kit (Tiangen Biotech Co. Ltd., Beijing, China). The FBS protein loading ratio was evaluated by the following equation: $q = (W_{Total} - W_{Sup})/(W_{GO}) \times 100\%$ (W_{Total}, W_{Sup}, and W_{GO} represented the total amount of protein, the amount of protein in the suspension, and the quantity of GO, respectively).

Additionally, the GO suspension (1 mg/mL) was mixed with BSA solution (1 mg/mL) at 37 °C for 2 h. After centrifugation at ~19000*g* for 10 min, the protein concentration of the supernatant was measured by Bradford Protein Assay Kit, and the capability of BSA adsorbed (*q*) on the GO face was calculated as the defined equation.

Cell Culture and Cytotoxicity Test. A549 cells were grown in RPMI-1640 (Invitrogen, Carlsbad, CA, USA) with 10% heat-inactivated fetal bovine serum and antibiotics (100 μg/mL streptomycin and 100 U/mL penicillin) at 37 °C under conditions of 5% CO_2. Cells were seeded in 24-well plates and grown overnight. When ~70% confluency was reached, fresh media containing MWNTs, GO, or FBS-coated GO suspension was added at different concentrations (0, 20, 40, 60, 80, and 100 μg/mL). In addition, some cell suspensions were generated with or without 1% FBS and 20 μg/mL GO or FBS-coated GO suspension. After incubation, 50 μL of 5 mg/mL Thiazolyl Blue tetrazolium bromide (MTT; Sigma-Aldrich, St. Louis, MO, USA) solution was added to each well of the 24-well plate, followed by additional 4 h incubation at 37 °C. These cells were then lysed with 10% acid sodium dodecyl sulfate (SDS; Sigma) solution. After centrifugation at ~19000*g* for 10 min, the absorbance of the supernatant was measured at 570 nm on a microplate reader (model 680; Bio-Rad Hercules, CA, USA).

TEM Characterization. A549 cells were incubated at 37 °C in 1% FBS/RPMI 1640 medium containing 100 μg/mL GO or FBS-coated GO nanosheets, with a final cell concentration of 10^5 per mL. After 2 h, A549 cells were collected and washed twice with PBS, then fixed with 2.5% glutaraldehyde. The fixed cells were washed with PBS, postfixed with 1% aqueous OsO_4 (Fluka Chemical Corp. of Sigma-Aldrich) for 1 h, and washed twice with PBS. The cells were dehydrated through an ethanol series (70% for 15 min, 90% for 15 min, and two times with 100% for 15 min) and embedded in Epon/Araldite resin (polymerization at 65 °C for 15 h). Thin sections (90 nm) containing the cells were placed on the grids, stained for 1 min each with 4% uranyl acetate (1:1 acetone/water) and 0.2% Raynolds lead citrate (in water), air-dried, and examined under a transmission electron microscope (JEM-1230; Jeol Ltd., Tokyo, Japan).

Acknowledgment. The first two authors, W.H. and C.P., contributed equally to this work. The authors appreciate the financial support from the NSFC (20725516, 90913014), MOST (2007CB936000), Ministry of Health (2009ZX10004-301), and Shanghai Municipal Commission for Science and Technology (0952 nm04600).

Supporting Information Available: The purification treatment and characterization of MWNTs and SWNTs, viability of A549 cells treated with FBS- or BSA-coated GO for 2 h, C1s X-ray photoelectron spectroscopy spectra of FBS-coated GO and GO, and AFM image of BSA-coated GO. This material is available free of charge *via* the Internet at http://pubs.acs.org.

REFERENCES AND NOTES

1. Ball, P. Roll up for the Revolution. *Nature* **2001**, *414*, 142–144.
2. Prerona, C.; Wei, Q.; Mostafa, A. E.; Mark, R. P. Delivery of Molecules into Cells Using Carbon Nanoparticles Activated by Femtosecond Laser Pulses. *Nat. Nanotechnol.* **2010**, *5*, 607–611.
3. Muoth, M.; Helbling, T.; Durrer, L.; Lee, S. W.; Roman, C.; Hierold, C. Hysteresis-free Operation of Suspended Carbon Nanotube Transistors. *Nat. Nanotechnol.* **2010**, *5*, 589–592.
4. Pech, D.; Brunet, M.; Durou, H.; Huang, P.; Mochalin, V.; Gogotsi, Y.; Taberna, P.-L.; Simon, P. Ultrahigh-Power Micrometre-sized Supercapacitors Based on Onion-Like Carbon. *Nat. Nanotechnol.* **2010**, *5*, 651–654.
5. Bae, S.; Kim, H.; Lee, Y.; Xu, X.; Park, J.-S.; Zheng, Y.; Balakrishnan, J.; Lei, T.; Ri Kim, H.; Song, Y. I.; *et al.* Roll-to-Roll Production of 30-Inch Graphene Films for Transparent Electrodes. *Nat. Nanotechnol.* **2010**, *5*, 574–578.
6. Ray, S. C.; Saha, A.; Jana, N. R.; Sarkar, R. Fluorescent Carbon Nanoparticles: Synthesis, Characterization, and Bioimaging Application. *J. Phys. Chem. C* **2009**, *113*, 18546–18551.
7. Jin, H.; Heller, D. A.; Kalbacova, M.; Kim, J.-H.; Zhang, J.; Boghossian, A. A.; Maheshri, N.; Strano, M. S. Detection of Single-Molecule H_2O_2 Signalling from Epidermal Growth Factor Receptor Using Fluorescent Single-Walled Carbon Nanotubes. *Nat. Nanotechnol.* **2010**, *5*, 302–309.
8. Rutherglen, C.; Jain, D.; Burke, P. Nanotube Electronics for Radio Frequency Applications. *Nat. Nanotechnol.* **2009**, *4*, 811–819.
9. Tang, Y. J.; Ashcroft, J. M.; Chen, D.; Min, G.; Kim, C.-H.; Murkhejee, B.; Larabell, C.; Keasling, J. D.; Chen, F. F. Charge-Associated Effects of Fullerene Derivatives on Microbial Structural Integrity and Central Metabolism. *Nano Lett.* **2007**, *7*, 754–760.
10. Cherukuri, P.; Bachilo, S. M.; Litovsky, S. H.; Weisman, R. B. Near-Infrared Fluorescence Microscopy of Single-Walled Carbon Nanotubes in Phagocytic Cells. *J. Am. Chem. Soc.* **2004**, *126*, 15638–15639.
11. Liu, Z.; Cai, W.; He, L.; Nakayama, N.; Chen, K.; Sun, X.; Chen, X.; Dai, H. *In vivo* Biodistribution and Highly Efficient Tumour Targeting of Carbon Nanotubes in Mice. *Nat. Nanotechnol.* **2007**, *2*, 47–52.
12. Keren, S.; Zavaleta, C.; Cheng, Z.; de La Zerda, A.; Gheysens, O.; Gambhir, S. S. Noninvasive Molecular Imaging of Small Living Subjects Using Raman Spectroscopy. *Proc. Natl. Acad. Sci. U. S. A.* **2008**, *105*, 5844–5849.
13. Lu, F.; Gu, L.; Meziani, M. J.; Xin, W.; Luo, P. G.; Veca, L. M.; Cao, L.; Sun, Y.-P. Advances in Bioapplications of Carbon Nanotubes. *Adv. Mater.* **2009**, *21*, 139–152.
14. Rui, M.-M.; Eisei, N.; Hiroyuki, I.; Waka, N.; Koji, O.; Kent, D.; Takeshi, S.; Tetsuro, I.; Tatsuya, H.; Eiichi, N. *In vivo* Gene Delivery by Cationic Tetraamino Fullerene. *Proc. Natl. Acad. Sci. U. S. A.* **2010**, *107*, 5339–5344.
15. Liu, Z.; Winters, M.; Holodniy, M.; Dai, H. siRNA Delivery into Human T Cells and Primary Cells with Carbon-Nanotube Transporters. *Angew. Chem., Int. Ed.* **2007**, *46*, 2023–2027.
16. Yu, S.-J.; Kang, M.-W.; Chang, H.-C.; Chen, K.-M.; Yu, Y.-C. Bright Fluorescent Nanodiamonds: No Photobleaching and Low Cytotoxicity. *J. Am. Chem. Soc.* **2005**, *127*, 17604–17605.
17. Welsher, K.; Liu, Z.; Daranciang, D.; Dai, H. Selective Probing and Imaging of Cells with Single-Walled Carbon Nanotubes as Near-Infrared Fluorescent Molecules. *Nano Lett.* **2008**, *8*, 586–590.
18. Fu, C.-C.; Lee, H.-Y.; Chen, K.; Lim, T.-S.; Wu, H.-Y.; Lin, P.-K.; Wei, P.-K.; Tsao, P.-H.; Chang, H.-C.; Fann, W. Characterization and Application of Single Fluorescent Nanodiamonds as Cellular Biomarkers. *Proc. Natl. Acad. Sci. U. S. A.* **2007**, *104*, 727–732.
19. Kim, K. S.; Zhao, Y.; Jang, H.; Lee, S. Y.; Kim, J. M.; Kim, K. S.; Ahn, J.-H.; Kim, P.; Choi, J.-Y.; Hong, B. H. Large-Scale Pattern Growth of Graphene Films for Stretchable Transparent Electrodes. *Nature* **2009**, *457*, 706–710.
20. Schedin, F.; Geim, A. K.; Morozov, S. V.; Hill, E. W.; Blake, P.; Katsnelson, M. I.; Novoselov, K. S. Detection of Individual Gas Molecules Adsorbed on Graphene. *Nat. Mater.* **2007**, *6*, 652–655.
21. Wang, X.; Zhi, L.; Tsao, N.; Tomović, Z. e.; Li, J.; Mülen, K. Transparent Carbon Films as Electrodes in Organic Solar Cells. *Angew. Chem., Int. Ed.* **2008**, *47*, 2990–2992.
22. Geim, A. K.; Novoselov, K. S. The Rise of Graphene. *Nat. Mater.* **2007**, *6*, 183–191.

23. Neto, A. H. C.; Guinea, F.; Peres, N. M. R.; Novoselov, K. S.; Geim, A. K. The Electronic Properties of Graphene. *Rev. Mod. Phys.* **2009**, *81*, 109–154.
24. Geim, A. K. Graphene: Status and Prospects. *Science* **2009**, *324*, 1530–1534.
25. Lin, Y. M.; Dimitrakopoulos, C.; Jenkins, K. A.; Farmer, D. B.; Chiu, H. Y.; Grill, A.; Avouris, P. 100-GHz Transistors from Wafer-Scale Epitaxial Graphene. *Science* **2010**, *327*, 662.
26. Myung, S.; Park, J.; Lee, H.; Kim, K. S.; Hong, S. Ambipolar Memory Devices Based on Reduced Graphene Oxide and Nanoparticles. *Adv. Mater.* **2010**, *22*, 2045–2049.
27. Wan, Y.; Lin, Z.; Zhang, D.; Wang, Y.; Hou, B. Impedimetric Immunosensor Doped with Reduced Graphene Sheets Fabricated by Controllable Electrodeposition for the Non-labelled Detection of Bacteria. *Biosens. Bioelectron.* **2011**, *26*, 1959–1964.
28. Akhavan, O.; Ghaderi, E. Photocatalytic Reduction of Graphene Oxide Nanosheets on TiO_2 Thin Film for Photoinactivation of Bacteria in Solar Light Irradiation. *J. Phys. Chem. C* **2009**, *113*, 20214–20220.
29. Liu, Z.; Robinson, J. T.; Sun, X.; Dai, H. PEGylated Nanographene Oxide for Delivery of Water-Insoluble Cancer Drugs. *J. Am. Chem. Soc.* **2008**, *130*, 10876–10877.
30. Sun, X.; Liu, Z.; Welsher, K.; Robinson, J.; Goodwin, A.; Zaric, S.; Dai, H. Nano-Graphene Oxide for Cellular Imaging and Drug Delivery. *Nano Res.* **2008**, *1*, 203–212.
31. Zhang, L.; Xia, J.; Zhao, Q.; Liu, L.; Zhang, Z. Functional Graphene Oxide as a Nanocarrier for Controlled Loading and Targeted Delivery of Mixed Anticancer Drugs. *Small* **2010**, *6*, 537–544.
32. Lu, C.-H.; Zhu, C.-L.; Li, J.; Liu, J.-J.; Chen, X.; Yang, H.-H. Using Graphene to Protect DNA from Cleavage during Cellular Delivery. *Chem. Commun.* **2010**, *46*, 3116–3118.
33. Wang, Y.; Li, Z.; Hu, D.; Lin, C.-T.; Li, J.; Lin, Y. Aptamer/Graphene Oxide Nanocomplex for *in situ* Molecular Probing in Living Cells. *J. Am. Chem. Soc.* **2010**, *132*, 9274–9276.
34. Yang, K.; Zhang, S.; Zhang, G.; Sun, X.; Lee, S.-T.; Liu, Z. Graphene in Mice: Ultrahigh *in vivo* Tumor Uptake and Efficient Photothermal Therapy. *Nano Lett.* **2010**, *10*, 3318–3323.
35. Nel, A.; Xia, T.; Mädler, L.; Li, N. Toxic Potential of Materials at the Nanolevel. *Science* **2006**, *311*, 622–627.
36. Sayes, C. M.; Liang, F.; Hudson, J. L.; Mendez, J.; Guo, W.; Beach, J. M.; Moore, V. C.; Doyle, C. D.; West, J. L.; Billups, W. E.; *et al*. Functionalization Density Dependence of Single-Walled Carbon Nanotubes Cytotoxicity *in vitro*. *Toxicol. Lett.* **2006**, *161*, 135–142.
37. Dumortier, H.; Lacotte, S.; Pastorin, G.; Marega, R.; Wu, W.; Bonifazi, D.; Briand, J.-P.; Prato, M.; Muller, S.; Bianco, A. Functionalized Carbon Nanotubes are Non-cytotoxic and Preserve the Functionality of Primary Immune Cells. *Nano Lett.* **2006**, *6*, 1522–1528.
38. Chen, H.; Müller, M. B.; Gilmore, K. J.; Wallace, G. G.; Li, D. Mechanically Strong, Electrically Conductive, and Biocompatible Graphene Paper. *Adv. Mater.* **2008**, *20*, 3557–3561.
39. Park, S.; Mohanty, N.; Suk, J. W.; Nagaraja, A.; An, J.; Piner, R. D.; Cai, W.; Dreyer, D. R.; Berry, V.; Ruoff, R. S. Biocompatible, Robust Free-Standing Paper Composed of a Tween/Graphene Composite. *Adv. Mater.* **2010**, *22*, 1736–1740.
40. Agarwal, S.; Zhou, X.; Ye, F.; He, Q.; Chen, G. C. K.; Soo, J.; Boey, F.; Zhang, H.; Chen, P. Interfacing Live Cells with Nanocarbon Substrates. *Langmuir* **2010**, *26*, 2244–2247.
41. Chang, Y.; Yang, S.-T.; Liu, J.-H.; Dong, E.; Wang, Y.; Cao, A.; Liu, Y.; Wang, H. *In vitro* Toxicity Evaluation of Graphene Oxide on A549 Cells. *Toxicol. Lett.* **2011**, *200*, 201–210.
42. Zhang, Y.; Ali, S. F.; Dervishi, E.; Xu, Y.; Li, Z.; Casciano, D.; Biris, A. S. Cytotoxicity Effects of Graphene and Single-Wall Carbon Nanotubes in Neural Phaeochromocytoma-Derived PC12 Cells. *ACS Nano* **2010**, *4*, 3181–3186.
43. Akhavan, O.; Ghaderi, E. Toxicity of Graphene and Graphene Oxide Nanowalls Against Bacteria. *ACS Nano* **2010**, *4*, 5731–5736.
44. Hu, W.; Peng, C.; Luo, W.; Lv, M.; Li, X.; Li, D.; Huang, Q.; Fan, C. Graphene-Based Antibacterial Paper. *ACS Nano* **2010**, *4*, 4317–4323.
45. Fan, H.; Wang, L.; Zhao, K.; Li, N.; Shi, Z.; Ge, Z.; Jin, Z. Fabrication, Mechanical Properties, and Biocompatibility of Graphene-Reinforced Chitosan Composites. *Biomacromolecules* **2010**, *11*, 2345–2351.
46. Guo, C. X.; Zheng, X. T.; Lu, Z. S.; Lou, X. W.; Li, C. M. Biointerface by Cell Growth on Layered Graphene-Artificial Peroxidase-Protein Nanostructure for *in situ* Quantitative Molecular Detection. *Adv. Mater.* **2010**, *22*, 5164–5167.
47. Feng, L.; Zhang, S.; Liu, Z. Graphene Based Gene Transfection. *Nanoscale* **2011**, *3*, 1252–1257.
48. Zhang, X.; Yin, J.; Peng, C.; Hu, W.; Zhu, Z.; Li, W.; Fan, C.; Huang, Q. Distribution and Biocompatibility Studies of Graphene Oxide in Mice after Intravenous Administration. *Carbon* **2011**, *49*, 986–995.
49. Wang, K.; Ruan, J.; Song, H.; Zhang, J.; Wo, Y.; Guo, S.; Cui, D. Biocompatibility of Graphene Oxide. *Nanoscale Res. Lett.* **2010**, *6*, 8.
50. Hummers, W. S.; Offeman, R. E. Preparation of Graphitic Oxide. *J. Am. Chem. Soc.* **1958**, *80*, 1339.
51. Dong, X.; Shi, Y.; Zhao, Y.; Chen, D.; Ye, J.; Yao, Y.; Gao, F.; Ni, Z.; Yu, T.; Shen, Z.; *et al*. Symmetry Breaking of Graphene Monolayers by Molecular Decoration. *Phys. Rev. Lett.* **2009**, *102*, 135501.
52. Magrez, A.; Kasas, S.; Salicio, V.; Pasquier, N.; Seo, J. W.; Celio, M.; Catsicas, S.; Schwaller, B.; Forró, L. Cellular Toxicity of Carbon-Based Nanomaterials. *Nano Lett.* **2006**, *6*, 1121–1125.
53. He, S.; Song, B.; Li, D.; Zhu, C.; Qi, W.; Wen, Y.; Wang, L.; Song, S.; Fang, H.; Fan, C. A Graphene Nanoprobe for Rapid, Sensitive, and Multicolor Fluorescent DNA Analysis. *Adv. Funct. Mater.* **2010**, *20*, 453–459.
54. Zuo, X.; He, S.; Li, D.; Peng, C.; Huang, Q.; Song, S.; Fan, C. Graphene Oxide-Facilitated Electron Transfer of Metalloproteins at Electrode Surfaces. *Langmuir* **2009**, *26*, 1936–1939.
55. Song, S.; Qin, Y.; He, Y.; Huang, Q.; Fan, C.; Chen, H. Functional Nanoprobes for Ultrasensitive Detection of Biomolecules. *Chem. Soc. Rev.* **2010**, *39*, 4234–4243.
56. Cedervall, T.; Lynch, I.; Lindman, S.; Bergg rd, T.; Thulin, E.; Nilsson, H.; Dawson, K. A.; Linse, S. Understanding the Nanoparticle-Protein Corona Using Methods to Quantify Exchange Rates and Affinities of Proteins for Nanoparticles. *Proc. Natl. Acad. Sci. U. S. A.* **2007**, *104*, 2050–2055.
57. Dell'Orco, D.; Lundqvist, M.; Oslakovic, C.; Cedervall, T.; Linse, S. Modeling the Time Evolution of the Nanoparticle-Protein Corona in a Body Fluid. *PloS One* **2010**, *5*, e10949.
58. Manna, S. K.; Sarkar, S.; Barr, J.; Wise, K.; Barrera, E. V.; Jejelowo, O.; Rice-Ficht, A. C.; Ramesh, G. T. Single-Walled Carbon Nanotube Induces Oxidative Stress and Activates Nuclear Transcription Factor-κB in Human Keratinocytes. *Nano Lett.* **2005**, *5*, 1676–1684.
59. Pulskamp, K.; Diabaté, S.; Krug, H. F. Carbon Nanotubes Show no Sign of Acute Toxicity but Induce Intracellular Reactive Oxygen Species in Dependence on Contaminants. *Toxicol. Lett.* **2007**, *168*, 58–74.
60. Shvedova, A. A.; Kisin, E. R.; Mercer, R.; Murray, A. R.; Johnson, V. J.; Potapovich, A. I.; Tyurina, Y. Y.; Gorelik, O.; Arepalli, S.; Schwegler-Berry, D.; *et al*. Unusual Inflammatory and Fibrogenic Pulmonary Responses to Single-Walled Carbon Nanotubes in Mice. *Am. J. Physiol. Lung Cell Mol. Physiol.* **2005**, *289*, L698–L708.
61. Hull, M. S.; Kennedy, A. J.; Steevens, J. A.; Bednar, A. J.; Weiss, J. C. A.; Vikesland, P. J. Release of Metal Impurities from Carbon Nanomaterials Influences Aquatic Toxicity. *Environ. Sci. Technol.* **2009**, *43*, 4169–4174.
62. Narayan, R. J.; Berry, C. J.; Brigmon, R. L. Structural and Biological Properties of Carbon Nanotube Composite Films. *Mater. Sci. Eng.-B* **2005**, *123*, 123–129.
63. Lopez, C. F.; Nielsen, S. O.; Moore, P. B.; Klein, M. L. Understanding Nature's Design for a Nanosyringe. *Proc. Natl. Acad. Sci. U. S. A.* **2004**, *101*, 4431–4434.
64. Mu, Q.; Broughton, D. L.; Yan, B. Endosomal Leakage and Nuclear Translocation of Multiwalled Carbon Nanotubes: Developing a Model for Cell Uptake. *Nano Lett.* **2009**, *9*, 4370–4375.

65. Kang, S.; Pinault, M.; Pfefferle, L. D.; Elimelech, M. Single-Walled Carbon Nanotubes Exhibit Strong Antimicrobial Activity. *Langmuir* **2007**, *23*, 8670–8673.
66. Kang, S.; Herzberg, M.; Rodrigues, D. F.; Elimelech, M. Antibacterial Effects of Carbon Nanotubes: Size Does Matter!. *Langmuir* **2008**, *24*, 6409–6413.
67. De, M.; Rana, S.; Akpinar, H.; Miranda, O. R.; Arvizo, R. R.; Bunz, U. H. F.; Rotello, V. M. Sensing of Proteins in Human Serum Using Conjugates of Nanoparticles and Green Fluorescent Protein. *Nat. Chem.* **2009**, *1*, 461–465.
68. Casals, E.; Pfaller, T.; Duschl, A.; Oostingh, G. J.; Puntes, V. Time Evolution of the Nanoparticle Protein Corona. *ACS Nano* **2010**, *4*, 3623–3632.
69. Zhu, Y.; Li, W.; Li, Q.; Li, Y.; Li, Y.; Zhang, X.; Huang, Q. Effects of Serum Proteins on Intracellular Uptake and Cytotoxicity of Carbon Nanoparticles. *Carbon* **2009**, *47*, 1351–1358.
70. Zhu, Y.; Ran, T.; Li, Y.; Guo, J.; Li, W. Dependence of the Cytotoxicity of Multi-Walled Carbon Nanotubes on the Culture Medium. *Nanotechnology* **2006**, *17*, 4668.
71. Sayes, C. M.; Fortner, J. D.; Guo, W.; Lyon, D.; Boyd, A. M.; Ausman, K. D.; Tao, Y. J.; Sitharaman, B.; Wilson, L. J.; Hughes, J. B.; *et al*. The Differential Cytotoxicity of Water-Soluble Fullerenes. *Nano Lett.* **2004**, *4*, 1881–1887.